Madhwesh et al. International Journal of Mechanical and Materials Engineering (2021) 16:5
https://doi.org/10.1186/s40712-021-00127-5

International Journal of Mechanical and Materials Engineering

ORIGINAL PAPER Open Access

Experimental investigations and empirical relationship on the influence of innovative hub geometry in a centrifugal fan for performance augmentation

N. Madhwesh, K. Vasudeva Karanth and N. Yagnesh Sharma*

Abstract

Background: One of the problem areas of fluid flow in the turbomachine is its inlet region, manifested by flow distortions due to the induced fluid swirl accompanied by improper flow incidence onto the impeller. Further, the hub forms one of the main components of many of the turbomachines and it is found that there has not been significant study on geometrical modifications of the same in centrifugal fans for augmented performance. This is partially due to designers trying to reduce the cost of the overall machine.

Objective: There is a scope for detailed parametric study and the present work involves an exploration of flow behavior by parametric variation of hub geometry in terms of both its shape and size.

Methods: Experiments are carried out in order to determine the importance of hub with different size and shapes. The geometric models of hemi-spherical and ellipsoidal hubs are considered for the analyses in the present study.

Results: An optimized ellipsoidal hub configuration is found to yield a relative improvement of about 7.5% for head coefficient and 7.7% increase in relative theoretical efficiency over the hub-less base configuration. Finally, correlations are developed for the optimized hub shape configurations.

Conclusion: It is revealed from experimental analysis that hub plays a vital role in streamlining the flow at the inlet to the centrifugal fan and augments its performance.

Keywords: Centrifugal fan, Ellipsoidal hub, Hemi-spherical hub, Flow guidance, Convergence, Relative theoretical efficiency

Introductionk

It is generally understood that the flow behavior at the entrance region of an impeller of the centrifugal fan is highly complex with pre-rotation, swirl, and strong fluid—boundary interactions. These behaviors result in not only improper incidence but also undesirable flow losses at the inlet zone of the impeller, causing a reduction in the overall efficiency of the fan. To capture the flow loss phenomena in the inlet swirling zone of the fan, a detailed experimental analysis is generally desired. Due to inlet flow distortions, it is essential to develop a suitable modification of inlet flow geometry to improve the flow characteristics. Many attempts have been made earlier by various researchers on inlet geometric interventions so as to alter the flow behavior for possible overall improvement of the fan.

Gancedo et al. (2018) described the effect of bleed slots on the enhancement of surge margin in a centrifugal compressor of turbocharger. They dealt with study of flow instabilities and its consequent effect of unstable

* Correspondence: nyagneshsharma@gmail.com
Department of Mechanical and Manufacturing Engineering, Manipal Institute of Technology, Manipal Academy of Higher Education, Manipal, Karnataka 576104, India

flow on compressor map especially at lower mass flow rates. It is found that by providing the bleed slot stability of the compressor gets improved. The flow patterns and the pressure fluctuations in a centrifugal pump with and without inlet guide vanes (IGV) were studied by Liu et al. (2018). They used inlet guide vanes of two and three dimensional nature for their study at various flow rate conditions. It is found in their study that the IGVs significantly minimize the pressure fluctuations. It is also revealed from their study that the amplitude of pressure fluctuations diminishes by about 22% and 45% respectively in 2D and 3D IGVs. The use of variable pitch inducers on the upstream side of the impeller was studied numerically and experimentally by Guo et al. (2017) to improve the anti-cavitation effect. It is observed from their study that with the increase in rotational speed, the static pressure is found to increase at both the inducer and the impeller. The authors stated that the variation of pressure at the inducer and the impeller is asymmetric in nature. Tamaki et al. (2016) tried to shift the compressor stability limit in a centrifugal compressor using finned inlet method. The study mainly focused on the effect of small fins at the inlet. It is concluded from their study that the inlet recirculation is prevented by the inlet fins. Liu et al. (2014) investigated the influence of bell mouth at inlet of semi-opened type axial fan on its flow behavior experimentally. They concluded that the pressure-rise near the best efficiency point becomes small with the decreasing bell mouth size.

Mistry and Pradeep (2014) performed experimental investigations on the hub-strong and tip-strong radial inflow distortion on a fan stage performance. Screens were provided at the upstream of the rotor to generate radial inflow distortions. At the inlet, both hub-strong and tip-strong radial inflow distortions were simulated by the authors. The two rotors were examined for inflow conditions to assess the performance. They found a reducing trend in overall performance of the fan in terms of pressure rise and efficiency by about 2 to 4% for the hub-strong radial distortion. Chen and Lei (2013) adopted ported shroud casing treatment method to improve the stability of centrifugal compressors in turbo charger applications. The authors analyzed the effect of a small quantum of fluid that was injected from impeller shroud recirculated into the impeller inlet. They found a good improvement in the blade loading for the ported shroud configuration. Further, they also reported that the shroud hinders the formation of shock waves and flow separation at the inlet. Liu et al. (2012) experimentally studied the influence of inlet geometry of impeller on overall flow behavior in a propeller fan. They incorporated three types of inlet geometries, with first type of impeller having completely covered blade tip, the second type with front 33% opened blade tip and the last one with front two-third portion opened. Analysis revealed that static pressure drops for the higher opened area of the blade tip. Luo et al. (2008) investigated the possible performance improvement of a centrifugal pump both experimentally and numerically by suitable modification of inlet geometry for pump impeller. They concluded that the uniform flow at the upstream of impeller inlet is helpful for improving cavitation performance of the pump. Bayomi et al. (2006) used unique concept of straighteners in the inlet duct of centrifugal fan for the purpose of elimination of inlet flow distortion, using the experimental analysis. They used two types of straighteners, namely, circular tubes and zigzag cross section, with different lengths. Tubes with various diameter values were also analyzed. They found an improvement of 12% in the flow margin as well as a reduction of about 4dB in the noise level for the circular tube configuration as compared to plain inlet configuration. The end wall of a compressor stator passage was examined experimentally by Johnson and Greitzer (1986). They adopted a method namely rotating slotted hub treatment. A smooth hub as well as axially skewed slotted hub was simulated by providing a whole field three dimensional transient velocity field in the vicinity of the hub. They found that axial skewed slots reduce the blockage drastically thereby reducing stalling flow coefficient. This results in an increased pressure rise and overall efficiency in their study.

It may be understood from a careful survey of literature detailed above that there has not been any significant research on the effect of geometric hub treatment in the inlet flow region for a centrifugal fan. The hub treatment has the potential to streamline the flow at the inlet of the impeller such that a smooth shock-less flow in this region considerably mitigates the flow distortions, thereby improving the overall static pressure gain across the impeller. This paper deals with an experimental study of inlet hub modifications for the performance improvement of centrifugal fan. It discusses elaborately parametric changes in the hub geometry for determining the best possible geometry for reduced losses occurring at the crucial inlet region.

Research methodology

Description of experimental test rig of centrifugal fan

The schematic proportionate drawing of the centrifugal fan adopted for present study is displayed in Fig. 1. The geometric information of the fan used closely matches the fan model used by Meakhail and Park (2005), such that validation of the results of the present study could be done.

The fan consists of four structural parts, namely, the inlet section, the bladed impeller, the vaned diffuser, and the rectangular volute casing. The inlet section with a

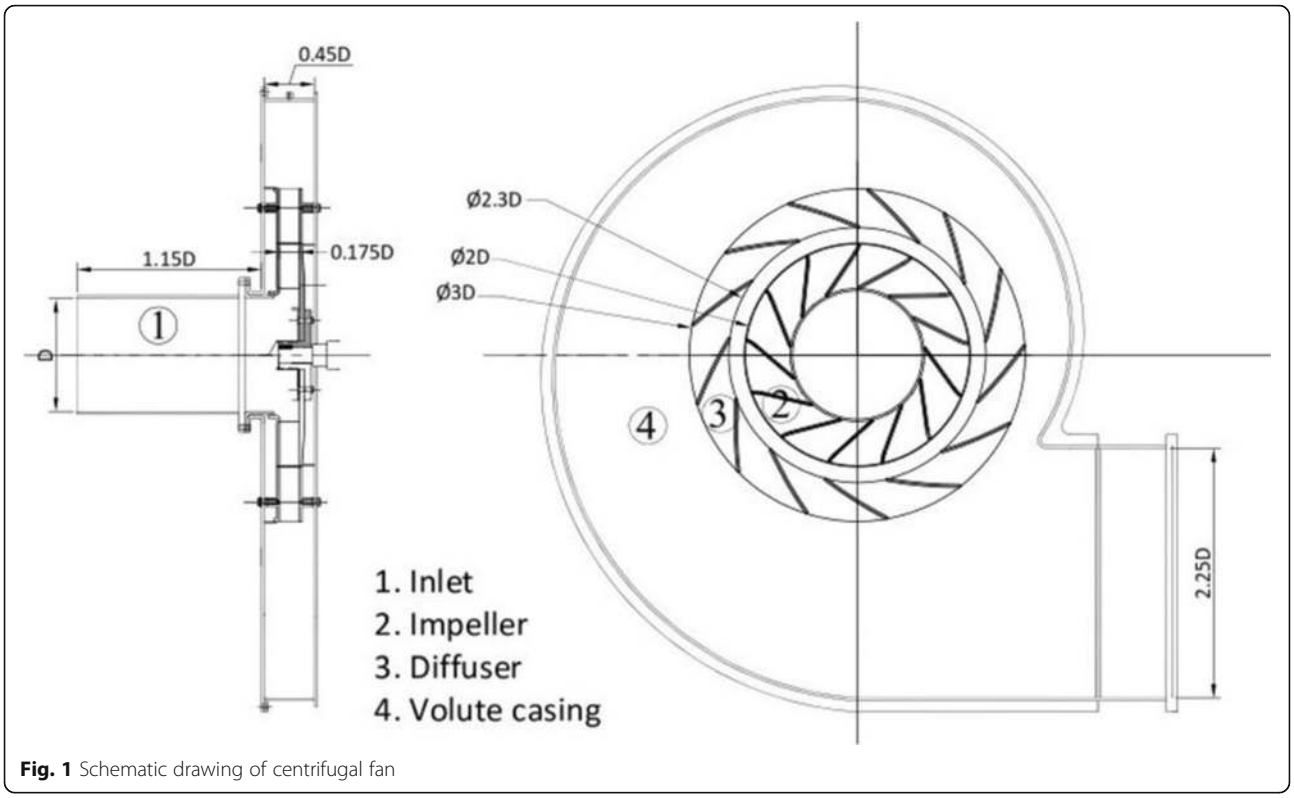

Fig. 1 Schematic drawing of centrifugal fan

diameter (D) of 200 mm is used as the reference dimension to represent all other dimensions of the fan. An entrance duct of 1.15 D is provided in order to ensure the profile of velocity conforming at the fan entry. The shrouded impeller is rearward swept and has thirteen equally spaced blades. The inlet and exit diameters of the impeller are 1.2 D and 2 D respectively. The blade angle of 30° is set for the impeller at its inlet whereas it is 76° at the exit. Each blade is having a rounded leading edge and has a thickness of 0.025 D. The impeller passage is 0.175 D wide in the axial direction. The impeller is followed by a diffuser having same number of blades, width, and blade thickness as that of the impeller.

The diffuser domain has inlet diameter of 2.3 D and exit diameter of 3 D. Inlet blade angle of 23° is maintained at the inlet of the diffuser while it is 38° at the blade exit. The diffuser passage width is same as that of impeller in the axial direction. A small clearance space up to 0.15 D is provided between the rotating impeller and stationary diffuser so that the transient turbulent flow is partially diminished before fluid enters the diffuser passages. The volute casing has a channel height of 0.45 D. The flange width is kept at 2.25 D at volute exit. Figures 2 and 3 show the experimental setup of centrifugal fan test rig and its close-up view respectively.

The experimental procedure consists of measurements of air flow rate (Q), static pressure, power input to obtain the overall efficiency. The experiments are repeated multiple number of times to get consistent output data of the fan. The standard performance graphs are then plotted using experimental values. High precision calibrated instruments are deployed to obtain reliable experimental data. Both static and stagnation pressures are recorded at the inlet section of the fan and at exit point of the diffuser by using digital manometer which has a resolution of 0.01 mm of water. The rotational speed of the fan is measured by a non-contact type digital tachometer that has a resolution of 1 RPM.

Experiments are conducted on the test rig initially, without the proposed appendage. This arrangement is considered as the hub-less base configuration in the present study. The fan which is driven by 3HP DC motor runs at a rated speed of 1500 RPM. A butterfly valve provided at the exit pipe is connected to the end flange of the volute chamber and is employed to regulate the air flow rate as shown in Fig. 4. The static and stagnation pressures are measured using pitot tube located at the exit pipe of the fan. It is also used to obtain the air exit velocity through a detachable traversing mechanism.

Determination of design point operation of the fan

A plot of overall efficiency (η_{ov}), as defined below in Eq. (1), corresponding to various volume coefficients for the hub-less base configuration is shown in Fig. 5. Due to

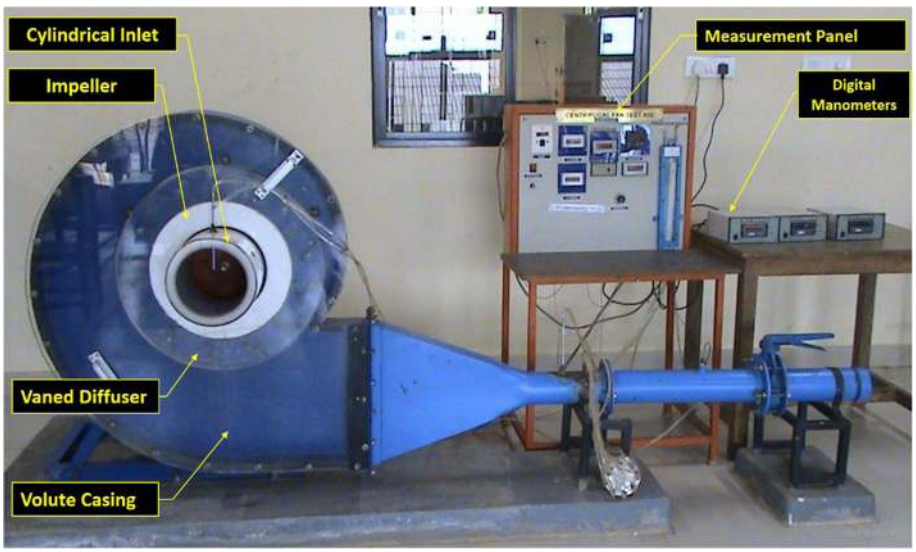

Fig. 2 Experimental set-up considered for the work

system limitations, the volume coefficient could not be increased beyond a maximum value of 0.051.

Overall efficiency (η_{ov}) as obtained from the experimental work is defined as the ratio of rate of static energy transfer from the rotor onto the fluid to the rate of actual electrical energy input to the fan. This is given by,

$$\eta_{ov} = \frac{(\Delta p_{st} \times Q)}{(\eta_t \times \eta_m \times P_{\text{in}})} \quad (1)$$

Where Δp_{st} is the difference between static pressures at fan exit (p_4) and fan inlet (p_1), η_t is transmission efficiency, η_m is motor efficiency, P_{in} is power input to motor.

It may be noted that the overall efficiency obtained from the experimental work is dependent on the input energy supplied by motor. The measurement of merely input electrical drive energy will not suffice as bearing and transmission losses are to be accounted for. Hence, to take care of these losses, motor and transmission efficiencies are taken 80% and 90% respectively, as per the panel specification on the motor.

It is observed that the overall efficiency has an increasing trend for the range of volume coefficients selected for the experiment. A peak overall efficiency of about 40.5% is achieved at a maximum volume coefficient of 0.051. Hence, the corresponding mass flow rate of 0.236 kg/s is taken as the design point operation of the fan.

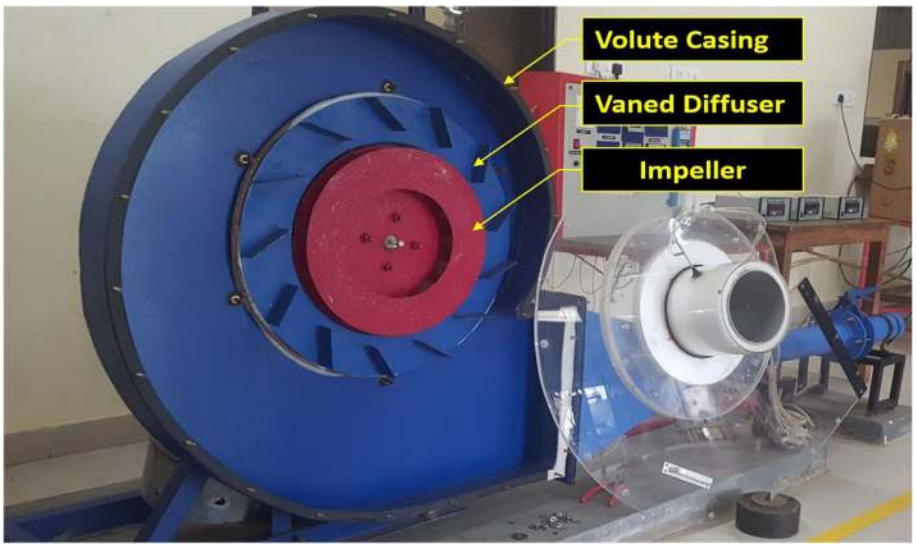

Fig. 3 Close-up view of the test rig

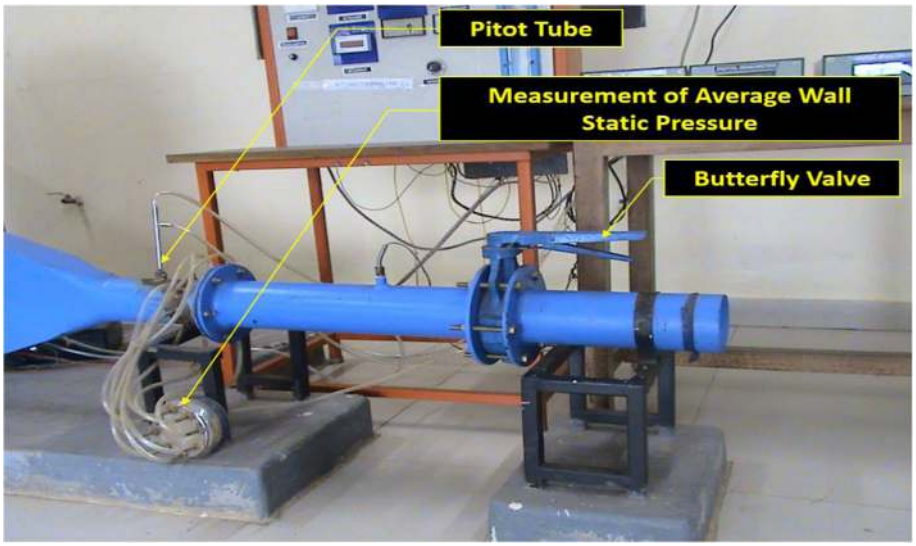

Fig. 4 Measurement arrangements at fan exit

Description of performance parameters used in the analysis

The performance variables namely volume and head coefficients are calculated for experimental work using Eqs. (2) and (3) respectively as shown below.

$$Volume\ coefficient, \phi = \left(\frac{Q}{\pi R_o^2 U_2}\right) \quad (2)$$

$$Head\ coefficient, \psi = \left(\frac{p_3}{\rho U_2^2}\right) \quad (3)$$

Where p_3 is static pressure at diffuser exit, U_2 is tangential speed of impeller at exit, ρ is density of air, R_0 is exit radius of the impeller.

So also, the relative theoretical efficiency (η_{Rt}) is found out using Eq. (4) and is defined as the ratio of specific

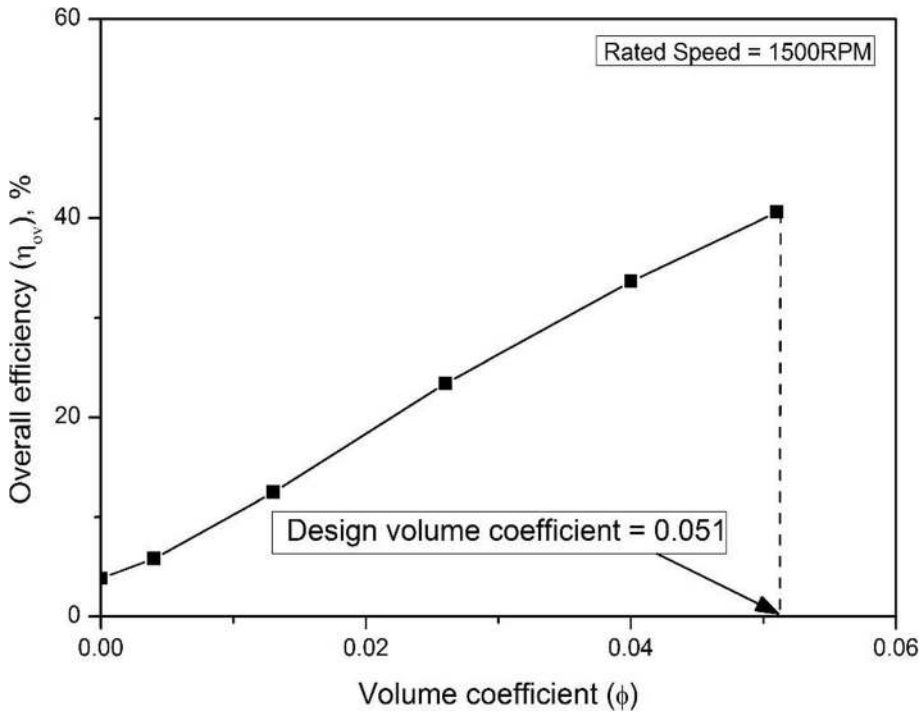

Fig. 5 Overall efficiency for various volume coefficients at rated speed

energy obtained from experimental work and that obtained through Euler's equation.

$$\eta_{Rt} = \left(\frac{H_{expt}}{H_{th}}\right) \tag{4}$$

Uncertainty analysis for the experimental work

It is obvious that the uncertainties are inevitable for the measurements in any experimental study. To estimate the measurement errors in the present experimental work, an uncertainty analysis is conducted as per the method suggested by Kline (1985).

The dependent variable chosen for uncertainty analysis is experimentally determined overall efficiency (η_{ov}). Piezometric head for obtaining rise in static pressure across the fan (y_1 mm of water), flow rate of air (y_2 mm of water), and the wattage input to the DC motor to drive fan (IP) are considered to be the measuring variables for the uncertainty analysis. Table 1 indicates the values of uncertainty corresponding to chosen measurement variables.

The uncertainty in the measurement of overall efficiency is obtained from the expression deduced by Kline (1985) and is given by,

$$U_{\eta_{ov}} = \left[\sum_{i=1}^{j}\left(\frac{\partial \eta_{ov}}{\partial y_i}U_{y_i}\right)^2 + 2\sum_{i=1}^{j-1}\sum_{k=i+1}^{j}\left(\frac{\partial \eta_{ov}}{\partial y_i}\right)\left(\frac{\partial \eta_{ov}}{\partial y_k}\right)U_{y_{ik}}\right]^{\frac{1}{2}} \tag{5}$$

where,

$$\eta_{ov} = \mathrm{f}\,(\mathrm{y}_1,\ \mathrm{y}_2,\ \mathrm{IP}) \tag{6}$$

It is found from Eq. (5) and Table 1 that the uncertainty value for the experimentally determined overall efficiency is within the limit of ±1.4%.

Description of various hub geometries adopted for the experiment

Generally, the fluid enters the impeller with a sharp and sudden change of direction from axial to meridional with the attendant flow losses for the hub-less base configuration as shown in Fig. 6.

The objective of this analysis is to examine the flow characteristics with variable hub geometry by providing either hemi-spherical or ellipsoidal shaped hub configurations as shown in Figs. 7 and 8 respectively. Experiments for both hemi-spherical-shaped hub (Fig. 7) and ellipsoidal-shaped hub (Fig. 8) configurations are performed to bring out the essential flow characteristics in each case vis-à-vis the hub-less base configuration. Figures 7b and 8b show the respective wooden models of hub fabricated for the experimental work. This wooden hub is fully secured to the back plate of the impeller and rotates along with the impeller.

The geometric parameter used for effecting the variations is expressed in terms of either spheroidal hub ratio (R_S) for hemi-spherical hub configurations or ellipsoidal hub ratio (R_E) for the ellipsoidal hub configurations. These ratios are non-dimensionalized in terms of entrance duct radius (r) as given in Eqs. (7) and (8) respectively.

$$\text{Spheroidal } \textit{hub} \text{ ratio, } R_S = \frac{\textit{Hub} \text{ radius}}{\text{Entrance duct radius}} = \frac{r_h}{r} \tag{7}$$

$$\text{Ellipsoidal } \textit{hub} \text{ ratio, } R_E = \frac{\text{Axial } \textit{hub} \text{ length}}{\text{Entrance duct radius}} = \frac{l_h}{r} \tag{8}$$

The values of spheroidal hub ratio and ellipsoidal hub ratio used in the analysis are tabulated in Table 2. Height of the ellipsoidal hub in the meridional direction (d) is obtained through optimization of hemi-spherical hub geometry as explained further in the "Effect of hemi-spherical hub configurations on the fan performance" section.

Results and discussion

The results of the experimental study are detailed in this section. The performance is carried out to obtain main and operating characteristics for different hub geometry configurations. Thus, the following discussion takes into account overall efficiency, head coefficient, and relative theoretical efficiency corresponding to chosen volume coefficients at the rated speed for hub-less base configuration as well as two-hub geometry configurations.

Effect of hemi-spherical hub configurations on the fan performance

Effect on overall efficiency

Figure 9 shows the variation of overall efficiency of the fan for various hemi-spherical hub configurations shown in Table 2. It is found that the presence of the hub

Table 1 Experimental uncertainties for the measuring variables

Measurement variables	Nomenclature	Expected uncertainty level of measurement variables
Static pressure rise	y_1 (mm)	$U_{y_1} = \pm 0.01$ mm of water
Air flow rate	y_2 (mm)	$U_{y_2} = \pm 0.01$ mm of water
Wattage input	IP (W)	$U_{IP} = \pm 0.25$ Watts

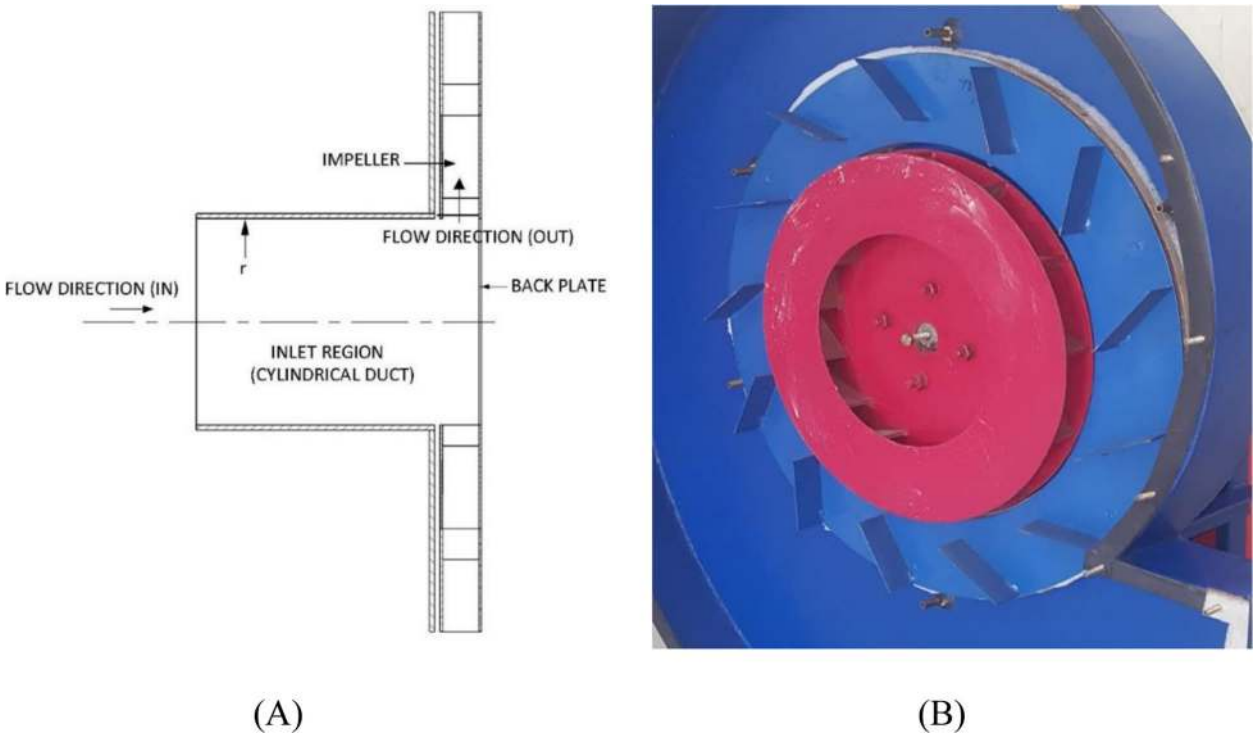

Fig. 6 Geometric configuration for the hub-less base configuration

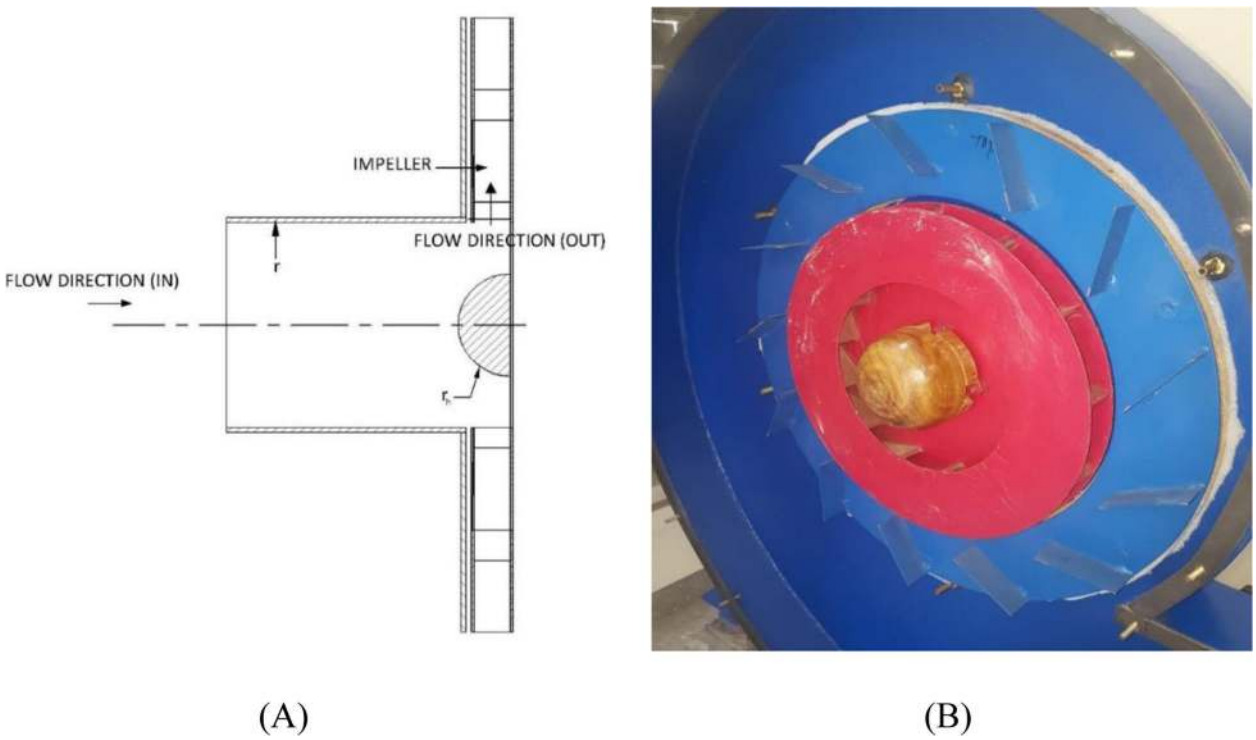

Fig. 7 Geometric configuration for the hemi-spherical hub configuration

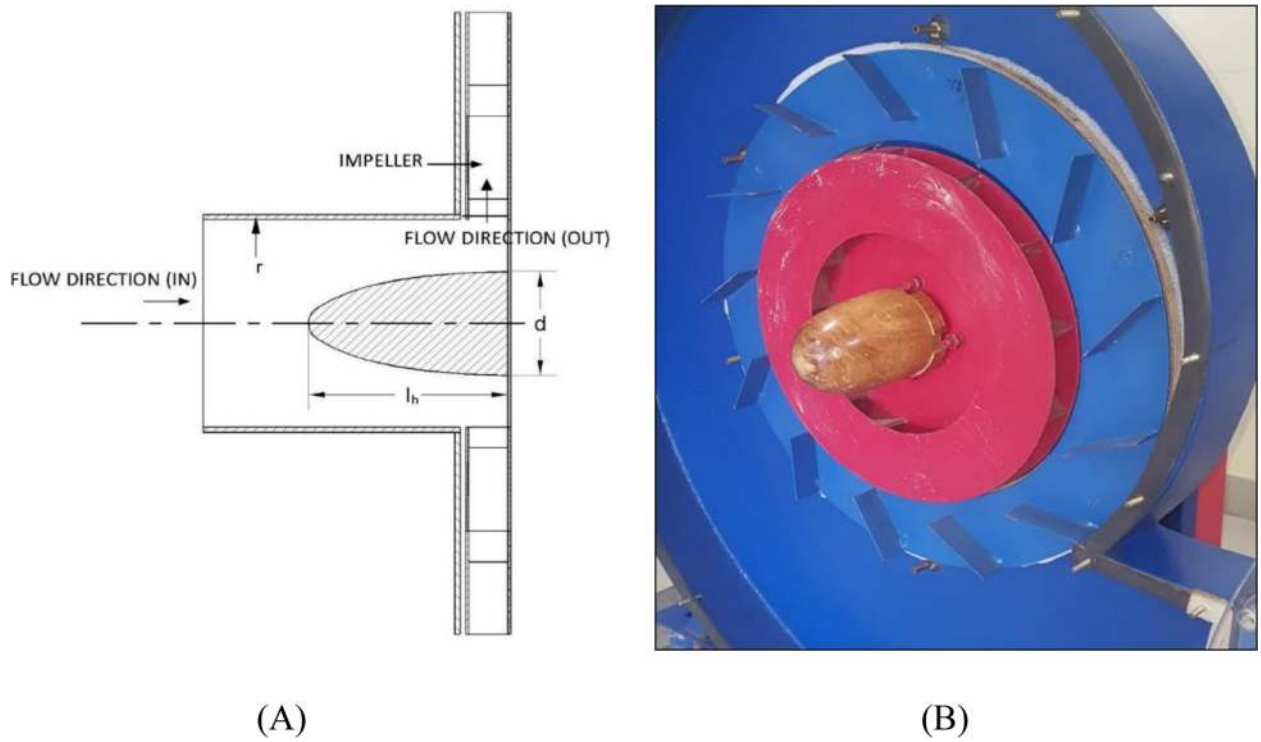

Fig. 8 Geometric configuration for the ellipsoidal hub configuration

improves the performance of the fan in terms of its overall efficiency at all volume coefficients. This is obviously because of the fact that basically hub provides better guidance for the flow of air at fan inlet in comparison to the hub-less configuration at corresponding volume coefficients. In general, it is observed that, on an average, there is an improvement in overall efficiency of about 2.6% for various hemi-spherical hub configurations over the hub-less base configuration at design volume coefficient as can be seen from the plot.

However, it is discernable that the hemi-spherical hub configuration S3 yields comparatively a higher overall efficiency of the fan at all volume coefficients. It is reasoned that this configuration is facilitating in re-laminarising the flow at the fan inlet which reduces inlet flow losses significantly and leads to static pressure improvement. Hence, hemi-spherical hub configuration S3 is considered as a useful optimum configuration for enhanced performance as regards to overall efficiency.

Further, the configurations S4 and S5 yield a lower overall efficiency when compared to S3 configuration. This is because of the possible constricted entry at the inlet due to protruding hub that could cause an accelerated flow resulting in flow losses.

Effect on main characteristics

The main characteristics for hemi-spherical hub configurations vis-a-vis the hub-less base configuration are depicted in Fig. 10. It is found that as the volume coefficient increases head coefficient decreases corroborating

Table 2 Configurations of hub arrangements

Hemi-spherical hub			Ellipsoidal hub		
Hub radius r_h (mm)	Configuration name	Spheroidal hub ratio	Hub length l_h (mm)	Configuration name	Ellipsoidal hub ratio
0.00	Hub-less base	0.00	0.00	Hub-less base	0.00
30.00	S1	0.30	30.00	E1	0.30
40.00	S2	0.40	50.00	E2	0.50
50.00	S3	0.50	70.00	E3	0.70
60.00	S4	0.60	90.00	E4	0.90
70.00	S5	0.70	110.00	E5	1.10
			130.00	E6	1.30

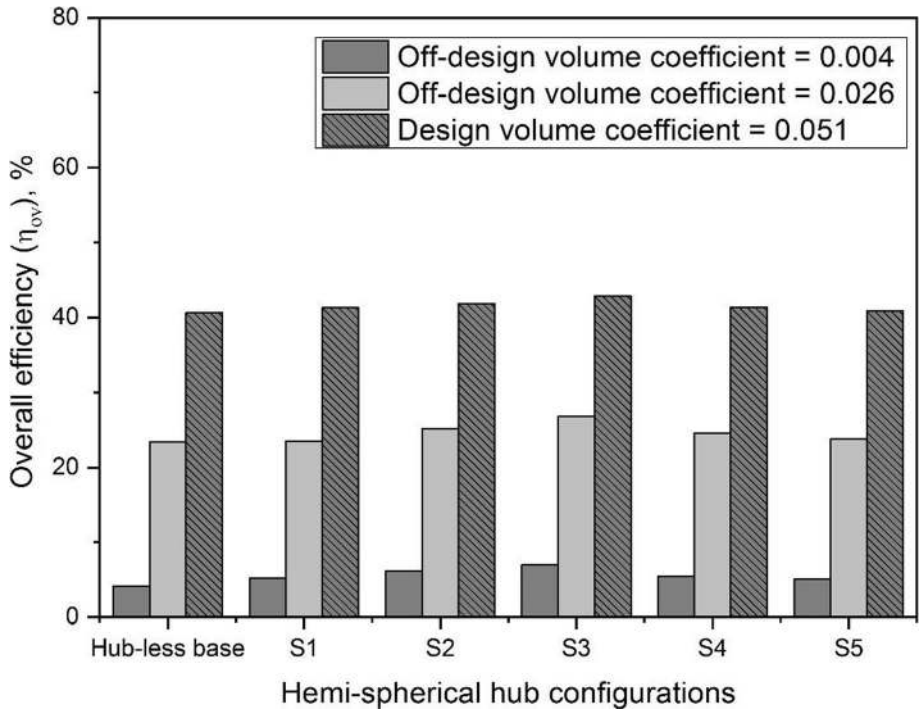

Fig. 9 Overall efficiency for hemi-spherical hub configurations for various volume coefficients

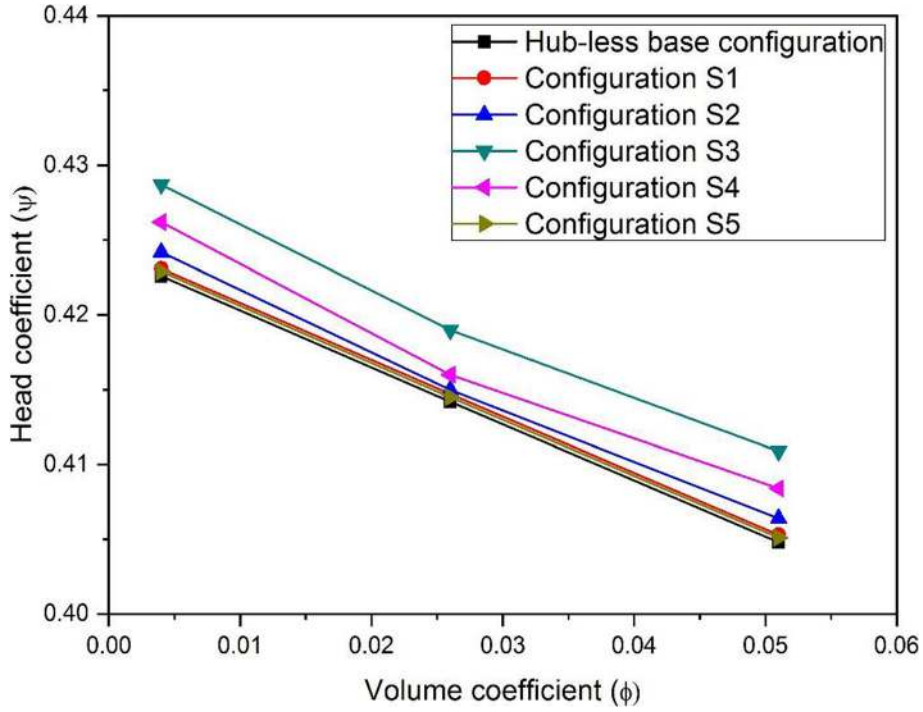

Fig. 10 Head coefficient for hemi-spherical hub configurations for various volume coefficients

the theoretical trend required for a typical backward curved impeller. It is found that, for any of the hub configurations when compared to hub-less base configuration, the head coefficient seems to be higher at all volume coefficients. In general, it is observed that there is relatively a higher value of head coefficient of about 0.6% over the hub-less base configuration, on an average, at design point volume coefficient.

It is interesting to observe that S3 configuration also has a higher head coefficient value at all volume coefficients as was the case for overall efficiency. It is clear that with this hemi-spherical configuration, flow admittance into the inlet region near the radial bend is smoother with little or no turbulence thereby improving the energy transfer process. An improvement of about 1.4% in head coefficient for the hemi-spherical hub configuration S3 vis-à-vis the hub-less base configuration for the range of volume coefficients is seen from Fig. 10.

This is due to the fact that the hemi-spherical hub contravenes the effect of stalling that is generally expected for the hub-less base model. This also ensures a relatively better guidance over the smoother surface of the hemi-spherical hub. As a consequence, a more streamlined flow of air enters the impeller and losses relatively minimized. This results in better head coefficient for the hub configuration S3 when compared with hub-less base model.

Effect on operating characteristics

To understand the operating behavior of the hub-less base model vis-à-vis various hub configurations, a relative theoretical efficiency is defined as given in Eq. (4). Figure 11 clearly shows the variation of relative theoretical efficiency for hub-less base model and other hub configurations at various values of volume coefficients. It is found that for all the hub configurations compared to hub-less base configuration there is an average improvement in relative theoretical efficiency by about 0.8% corresponding to the design point operation.

Not surprisingly, S3 configuration found to be the optimum hub configuration that has a higher relative theoretical efficiency of about 2.4% when compared to hub-less configuration. The reason for this being the same as was stated earlier in the "Effect on overall efficiency" and the "Effect on main characteristics" sections.

Effect of ellipsoidal hub configurations on the fan performance

Effect on overall efficiency

The variation of overall efficiency of the fan for various ellipsoidal hub configurations is shown in Fig. 12. It is found from Fig. 12 that there is an improvement in overall efficiency for the ellipsoidal hub configurations over that of the hub-less base configuration at all volume coefficients considered in the experimental work. This is attributed to the fact that the presence of the hub prevents the sudden change of direction from axial to radial

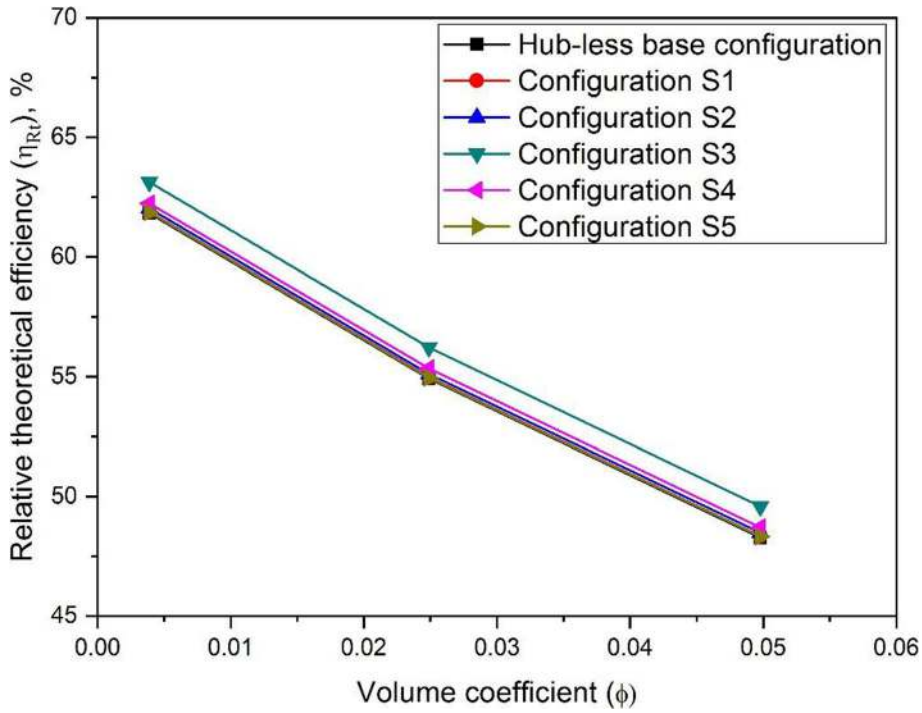

Fig. 11 Relative theoretical efficiency for hemi-spherical hub configurations for various volume coefficients

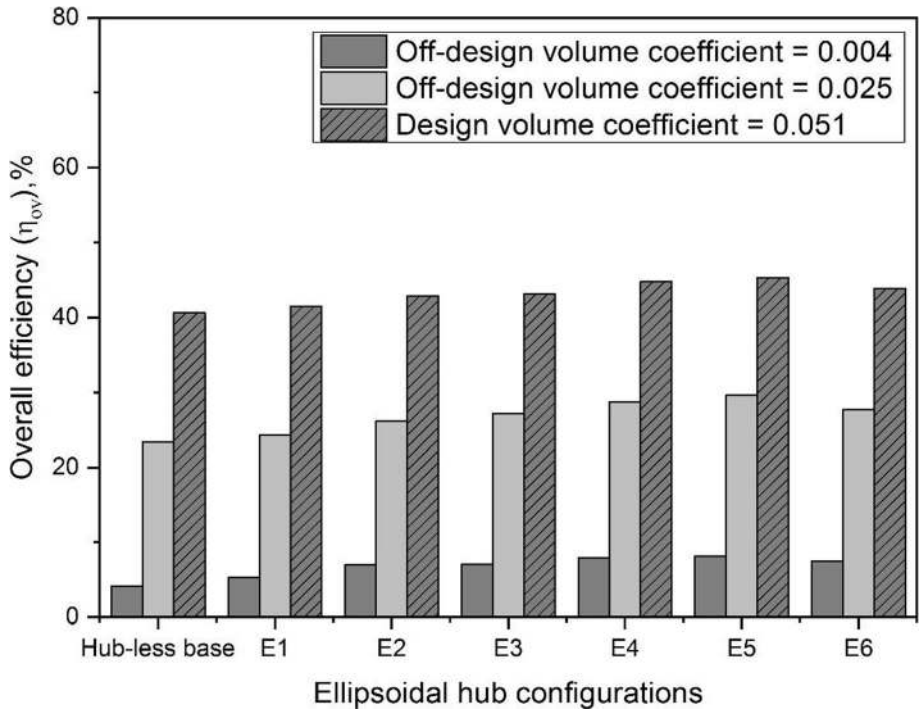

Fig. 12 Overall efficiency for ellipsoidal hub configurations for various volume coefficients

thereby minimizing the minor losses incurred due to this transition. Essentially the hub geometry leads to a streamlined through flow of air in the vicinity of eye of the impeller when compared with hub-less base configuration. An average improvement of about 7.3% is observed for various ellipsoidal hub configurations over the hub-less configuration at design point operation of the fan.

Interestingly, it is also seen from Fig. 12 that hub configuration E5 yields relatively higher overall efficiency of the fan at all volume coefficients used in the study. The reason for this improvement is stated as follows.

It is reasoned that for the configuration E5, the convergence of flow over the hub surface seems to be optimum. This helps in streamlining the flow in the constricted passage effectively. As a result, there could be an optimum gradual change in flow direction along the annular passage between the hub and inlet casing. The combined effect of optimum convergence and smoother flow transition relatively lowers the accountable incident losses; thereby, performance in terms of overall efficiency is comparatively higher for ellipsoidal hub configuration E5 over other configurations.

For ellipsoidal hub configurations built with lower axial hub length (configurations E1, E2, E3, and E4), there is a possibility of rapid rise in the velocity almost near the entrance region of the impeller due to converging annular passage. This results in streamlining of the flow in the vicinity of eye region. Also, the jet type of flow is emerging out of inlet region onto the impeller and hence there may not be scope for a gradual change in the direction of fluid flow. Hence, due to dominating effect of convergence over the flow guidance, performance in terms of overall efficiency improves but marginally.

Contrastingly, for the ellipsoidal hub with larger hub length (configuration E6), flow traverses a relatively longer annular distance and then takes a turn into the radial direction. Combined effect of this is that there is associated skin friction loss in the annular region. The flow also suffers a turning loss due to poor guidance at the inlet to the impeller because of the hub geometry. Thus, this configuration contributes to higher flow losses which render this configuration not suitable when compared to other configurations.

Effect on main characteristics

The main characteristics for ellipsoidal hub configurations in comparison with hub-less base configuration are shown in Fig. 13. It is discernable that hub configurations are found to yield relatively higher head coefficient values when compared with the hub-less base configuration at all volume coefficients. An average improvement of about 3.6% is observed for hub configurations over the hub-less base configuration at design point.

Again, configuration E5 is found to be the optimum configuration in terms of head coefficient. This may be reasoned as follows. Configuration E5 provides adequate

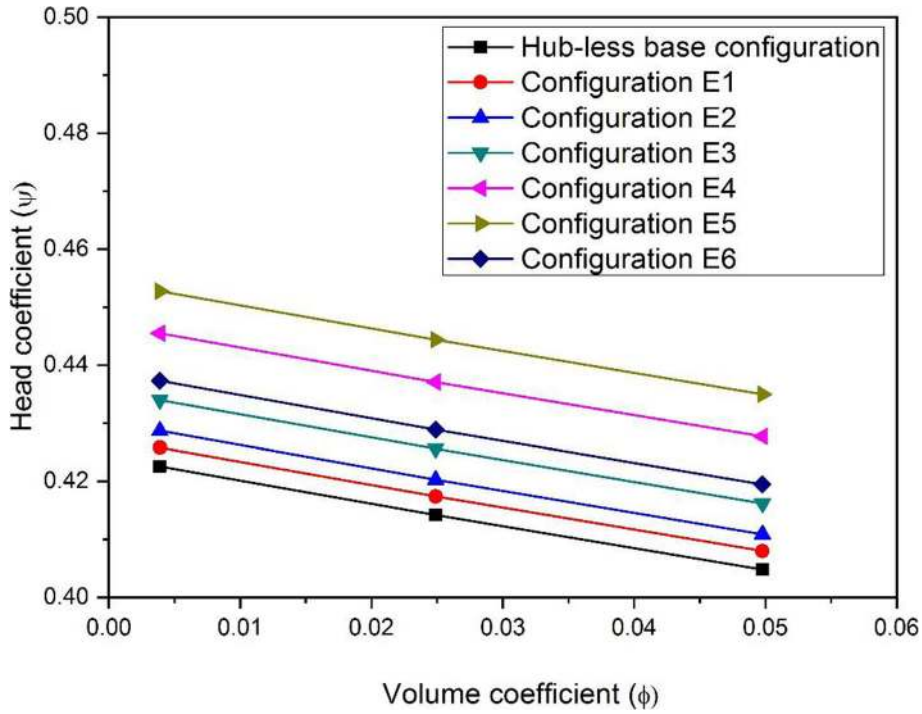

Fig. 13 Head coefficient for ellipsoidal hub configurations for various volume coefficients

convergence over the hub surface and enters the impeller with minimum incidence and friction losses. This helps in bettering the head coefficient by about 7.5% for configuration E5 over the hub-less base configuration as seen from Fig. 13.

Effect on operating characteristics

Relative theoretical efficiency is plotted for ellipsoidal hub configurations vis-à-vis hub-less base configuration to quantify the beneficial effects of hub and is depicted in Fig. 14. For various values of volume coefficients adopted in the analysis, it is revealed that all the hub configurations are found to deliver better operating characteristics for the fan. An average improvement of about 3.7% is observed in relative theoretical efficiency for hub configurations over the hub-less base model at design point.

However, configuration E5 seems to yield relatively higher relative theoretical efficiency when compared to other ellipsoidal hub configurations including hub-less base model. An average improvement of about 7.7% in relative theoretical efficiency is observed for configuration E5 over the hub-less base model at design point of the centrifugal fan. This improvement in relative theoretical efficiency clearly corroborates the improvements in overall efficiency as well as the main characteristics of the fan.

Comparison of optimum hemi-spherical and ellipsoidal hub configurations

It is interesting to compare the performance of the fan corresponding to the optimum hub geometry of hemi-spherical and ellipsoidal configurations. The overall efficiency and the relative theoretical efficiency are used for performance comparison.

The overall efficiency is plotted in Fig. 15 for optimum hemi-spherical hub configuration (S3) as well as optimum ellipsoidal hub configuration (E5), along with hub-less base configuration as benchmark. It is found that optimum ellipsoidal configuration (E5) shows a consistent improvement of about 11% in overall efficiency over that of the optimum hemi-spherical hub model (S3) for the range of volume coefficients considered.

Similarly, Fig. 15 also depicts the variation of relative theoretical efficiency for optimum hemi-spherical (S3) and ellipsoidal hub (E5) configurations. Again, the optimum ellipsoidal configuration E5 shows a significant improvement of about 3.5% in relative theoretical efficiency over that of the optimum hemi-spherical hub model (S3) for various volume coefficients used.

It is clear from the comparative study that configuration with ellipsoidal hub geometry E5 produces a better performance in terms of both the performance parameters. This may be established from the fact that a more streamlined flow in the vicinity of impeller eye region is obtained for this configuration when compared to

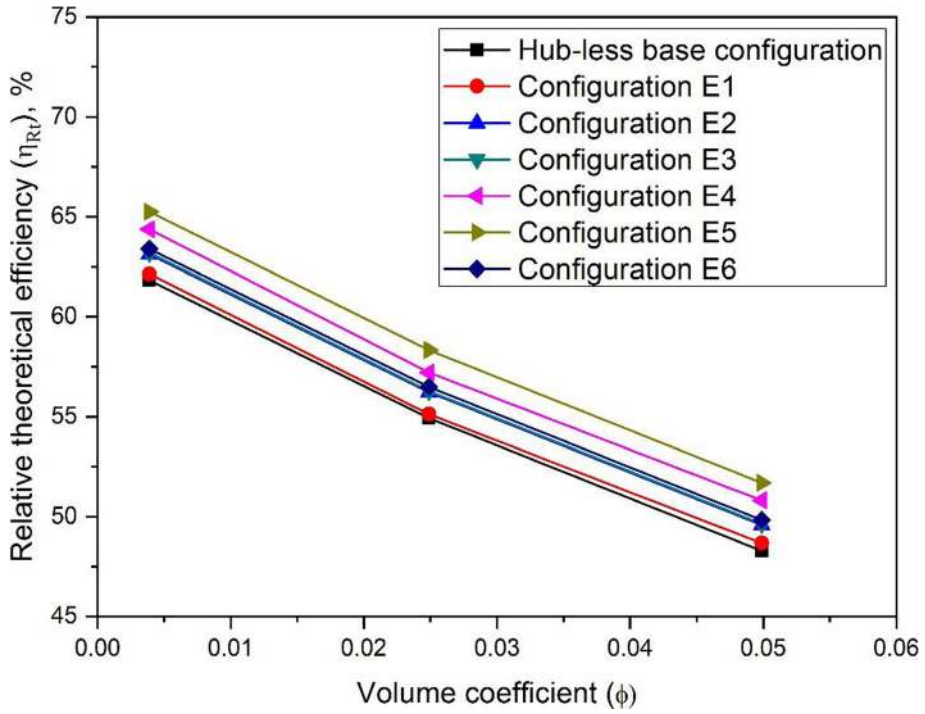

Fig. 14 Relative theoretical efficiency for various ellipsoidal hub geometry configurations for various volume coefficients

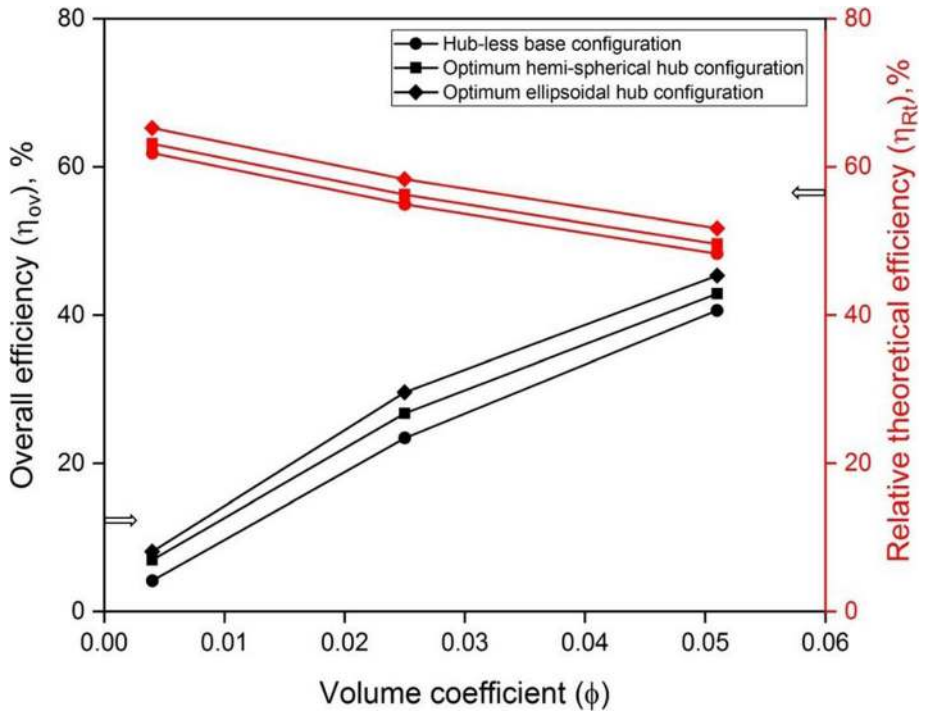

Fig. 15 Operating characteristics for optimized hemi-spherical and ellipsoidal hub geometries

optimized hemi-spherical hub model as well as hubless base model. Due to this, flow incidence losses are significantly reduced and the overall effect across the entire fan is an improvement in both overall efficiency and relative theoretical efficiency for this E5 configuration.

Hence, it is established in this study from a series of experiments on different hub configurations with parametric variation in geometry that as a design prescription a hub with ellipsoidal hub ratio of 1.1 corresponding to configuration E5 is found to be the best overall design that can be adopted with reasonable assurance of improved performance among the various configurations studied.

Development of correlations for the optimized hub-shape configuration

The results discussed in the "Effect on main characteristics" and the "Effect on operating characteristics" sections show that the fan performance characteristics, i.e., head coefficient (ψ) and relative theoretical efficiency (η_{Rt}), are significantly influenced by both volume coefficient (ϕ) and ellipsoidal hub ratio (R_E) considered in the study. Therefore, ψ and η_{Rt} can be expressed as functions of ϕ and R_E as given in Eqs. (9) and (10) respectively.

$$\psi = f(\phi, R_E) = C_1 \phi^a R_E^b \tag{9}$$

$$\eta_{Rt} = f(\phi, R_E) = C_2 \phi^m R_E^n \tag{10}$$

where C_1, C_2, a, b, m, and n are empirical constants.

Regression analysis of the experimentally obtained values has been performed to determine the constants in Eqs. (9) and (10). This analysis provides the exact relationships for ψ and η_{Rt}using least square fit and the correlations thus obtained are as shown in Eqs. (11) and (12) respectively.

$$\psi = 0.42\,\phi^{-0.015} R_E^{0.034} \tag{11}$$

$$\eta_{Rt} = 39.85\,\phi^{-0.088} R_E^{0.026} \tag{12}$$

Figures 16 and 17 show comparison of experimental and predicted values of head coefficient and relative theoretical efficiency for ellipsoidal hub geometry configurations. It can be seen from these parity plots that 95% of the predicted values of head coefficient and relative theoretical efficiency (calculated using Eqs. (11) and (12)) lies within ±5% of the experimentally obtained values as depicted by Singh et al. (2011).

The regression data of head coefficient for the correlation obtained in Eq. (11) has regression coefficient of 0.93 and average absolute deviation of 0.8% whereas the regression data of relative theoretical efficiency for the correlation obtained in Eq. (12) has regression coefficient of 0.89 and average absolute deviation of 4.9%. This depicts good agreement between predicted data and experimental data.

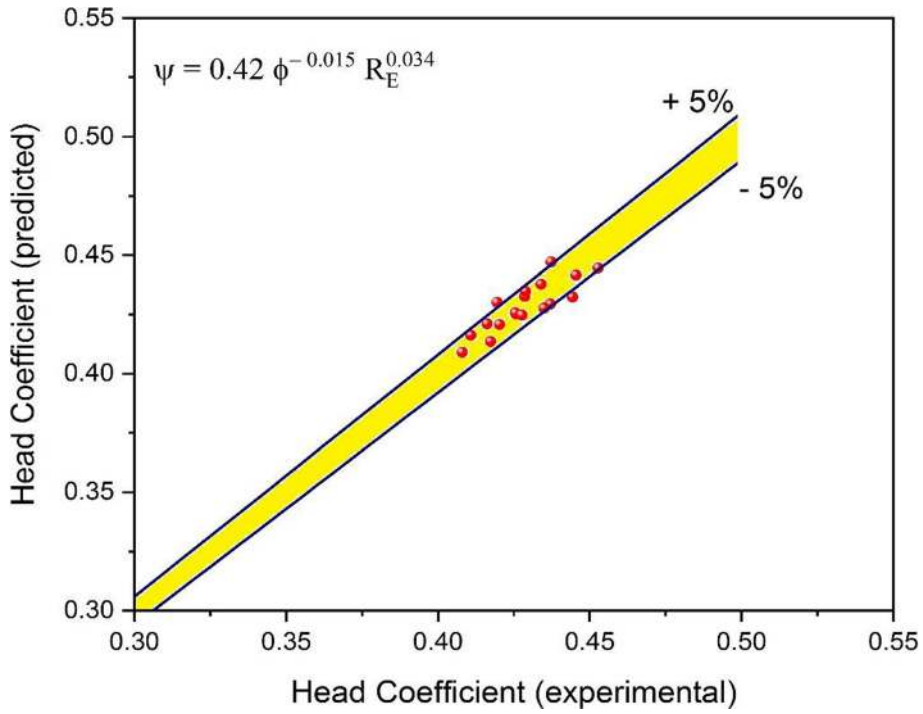

Fig. 16 Comparison of experimental and predicted values of head coefficient for ellipsoidal hub geometry configuration

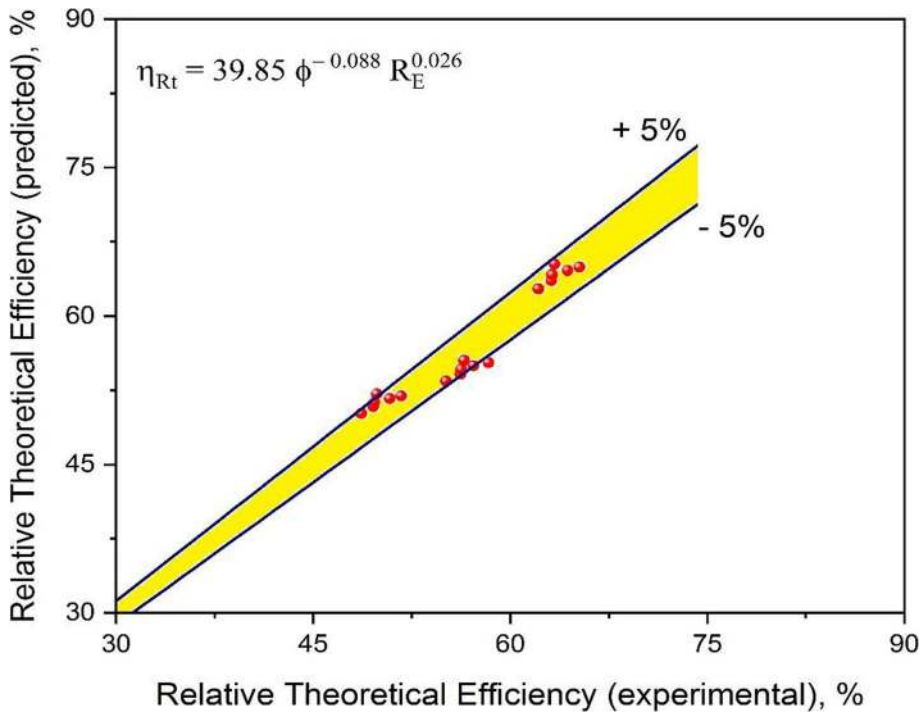

Fig. 17 Comparison of experimental and predicted values of relative theoretical efficiency for ellipsoidal hub geometry configuration

In conclusion, for the range of parameters investigated in the experimental work, the values of head coefficient as well as relative theoretical efficiency can be predicted with reasonable accuracy using the correlations developed in Eqs. (11) and (12) respectively.

Conclusion

It is shown that the hub provided at the inlet region has significant influence on the performance of centrifugal fan. The following conclusions are drawn from the present experimental work.

- It is found that both hemi-spherical and ellipsoidal hub geometry configurations contribute to higher overall efficiency as compared to hub-less base model at all volume coefficients considered in the study.
- Ellipsoidal hub configuration with ellipsoidal hub ratio of 1.1 contributed an improvement of about 7.5% in head coefficient and 7.7% in relative theoretical efficiency as compared to the hub-less base model for the range of volume coefficients adopted in the experiment.
- Hemi-spherical hub configuration with spheroidal hub ratio of 0.5 contributed to a higher head coefficient of about 1.4% and a higher relative theoretical efficiency of about 2.4% when compared to a hub-less base model at all volume coefficients.
- For hub configurations with ellipsoidal hub ratio beyond 1.1 as well as spheroidal hub ratio beyond 0.5, there was only a marginal improvement in terms of performance characteristics of the fan.
- Statistical correlations for head coefficient and relative theoretical efficiency have been developed as functions of volume coefficient and ellipsoidal hub ratio, and the correlations predict the values of head coefficient and relative theoretical efficiency with average absolute deviation of 0.8% and 4.9%, respectively.

Acknowledgements
The experimental facility for conducting this research work was provided by the Department of Mechanical and Manufacturing Engineering, Manipal Institute of Technology, Manipal Academy of Higher Education (MAHE), Manipal. The authors wish to express their gratitude and acknowledge the support provided by the institute in carrying out this research work.

Authors' contributions
Madhwesh N conducted experiments and built up correlations based on statistical analysis. K Vasudeva Karanth was the supervisor for the work and analyzed the experimental data. N Yagnesh Sharma was the overall coordinator of this research work and was instrumental in writing this article. All authors approved the manuscript.

Funding
There is no funding for this research work. However, authors have used a research test rig belonging to author's institute.

Availability of data and materials
The data that has been used in this research article is confidential. The datasets used and/or analyzed during the current study are available from the corresponding author on reasonable request.

Declarations

Competing interests

The authors declare that they have no known competing financial interests or personal relationships that could have appeared to influence the work reported in this paper.

Received: 15 September 2020 Accepted: 9 March 2021
Published online: 19 March 2021

References

Bayomi, N. N., Abdel Hafiz, A., & Osman, A. M. (2006). Effect of inlet straighteners on centrifugal fan performance. *Energy Conversion and Management*, *47*(18–19), 3307–3318. https://doi.org/10.1016/j.enconman.2006.01.003.

Chen, H., & Lei, V. M. (2013). Casing treatment and inlet swirl of centrifugal compressors. *Journal of Turbomachinery, Transactions of ASME*, *135*(4), 041010. https://doi.org/10.1115/1.4007739.

Gancedo, M., Guillou, E., & Gutmark, E. (2018). Effect of bleed slots on turbocharger centrifugal compressor stability. *International Journal of Heat and Fluid Flow*, *70*, 206–215. https://doi.org/10.1016/j.ijheatfluidflow.2017.12.007 Elsevier.

Guo, X. m., Zhu, Z.-c., Shi, G.-p., & Huang, Y. (2017). Effects of rotational speeds on the performance of a centrifugal pump with a variable-pitch inducer. *Journal of Hydrodynamics*, *29*(5), 854–862. https://doi.org/10.1016/S1001-6058(16)60797-7 Publishing House for Journal of Hydrodynamics.

Johnson, M. C., & Greitzer, E. M. (1986). Effects of slotted hub and casing treatments on compressor endwall flow fields. *Journal of Turbomachinery, Transactions of ASME*, *109*(3), 380–387. https://doi.org/10.1115/1.3262117.

Kline, S. J. (1985). The purposes of uncertainty analysis. *ASME Journal of Fluids Engineering*, *107*(2), 153–160. https://doi.org/10.1115/1.3242449.

Liu, M., Tan, L., & Cao, S. (2018). Influence of geometry of inlet guide vanes on pressure fluctuations of a centrifugal pump. *Journal of Fluids Engineering, Transactions of the ASME*, *140*(9), 1–13. https://doi.org/10.1115/1.4039714.

Liu, P., Shiomi, N., Kinoue, Y., Jin, Y.-z., & Setoguchi, T. (2012). Effect of inlet geometry on fan performance and flow field in a half-ducted propeller fan. *International Journal of Rotating Machinery*, *2012*, 1–9. https://doi.org/10.1155/2012/463585.

Liu, P., Shiomi, N., Kinoue, Y., Setoguchi, T., & Jin, Y.-z. (2014). Effect of inlet geometry on fan performance and inlet flow fields in a semi-opened axial fan. *International Journal of Fluid Machinery and Systems*, *7*(2), 60–67. https://doi.org/10.5293/IJFMS.2014.7.2.060.

Luo, X., Zhang, Y., Peng, J., Xu, H., & Yu, W. (2008). Impeller inlet geometry effect on performance improvement for centrifugal pumps. *Journal of Mechanical Science and Technology*, *22*(10), 1971–1976. https://doi.org/10.1007/s12206-008-0741-x.

Meakhail, T., & Park, S. O. (2005). A study of impeller-diffuser-volute interaction in a centrifugal fan. *Volume 5: Turbo Expo 2004, Parts A and B*, *127*(January 2005), 687–695. https://doi.org/10.1115/GT2004-53068.

Mistry, C., & Pradeep, A. M. (2014). Experimental study of the effect of radially distorted inflow on a contrarotating fan stage. *International Journal of Rotating Machinery.*, *2014*, 1–14. https://doi.org/10.1155/2014/503579.

Singh, S., Chander, S., & Saini, J. S. (2011). Heat transfer and friction factor correlations of solar air heater ducts artificially roughened with discrete V-down ribs. *Energy*, *36*(8), 5053–5064. https://doi.org/10.1016/j.energy.2011.05.052 Elsevier.

Tamaki, H., Unno, M., Tanaka, R., Yamaguchi, S., & Ishizu, Y. (2016). Enhancement of centrifugal compressor operating range by control of inlet recirculation with inlet fins. *Journal of Turbomachinery, Transactions of ASME*, *138*(10), 101010. https://doi.org/10.1115/1.4033187.

Publisher's Note